on a total-carbon basis may be low by one to two orders of magnitude. This would shift the average K_{oc} for atrazine to values in a range comparable to that observed in these experiments. Alternatively, the surface acidity of sediment or soil clay particles may have the effect observed here of decreasing the sorptive capacity of the organic matter.

These results suggest that natural colloids may be important in the transport of hydrophobic contaminants in the aquatic environment. Furthermore, the partitioning of solutes onto these colloids is highly dependent on bulk water characteristics, such as *p*H and salinity. The extreme *p*H dependence of these biopolymers also suggests that the sorptive properties of colloids must be studied under ambient conditions if meaningful data are to be obtained.

J. C. MEANS
Chesapeake Biological Laboratory, University of Maryland Center for Environmental and Estuarine Studies, Solomons 20688, and Department of Chemistry, University of Maryland, College Park 20742

R. WIJAYARATNE
Chesapeake Biological Laboratory

References and Notes

1. S. U. Khan and M. Schnitzer, *J. Environ. Sci. Health Part B* **13**, 229 (1978); H. D. Skipper and V. V. Volk, *Weed Sci.* **20**, 344 (1972); D. D. Kaufman and J. Blake, *Soil Biol. Biochem.* **2**, 73 (1970).
2. A. Siegel, in *Organic Compounds in Aquatic Environment*, S.D. Faust and J. V. Hunter, Eds. (Dekker, New York, 1971), p. 265; J. B. Andelman, in *Trace Metals and Metal-Organic Interactions in Natural Waters*, P. C. Singer, Ed. (Ann Arbor Science, Ann Arbor, Mich., 1974), p. 57; M. R. Hoffman, E. C. Yost, S. J. Eisenreich, W. J. Maier, *Environ. Sci. Technol.* **15**, 655 (1981).
3. A. C. Sigleo, G. R. Helz, W. H. Zoller, *Environ. Sci. Tech.* **14**, 673 (1980); A. C. Sigleo, T. C. Hoering, P. E. Hare, *Carnegie Inst. Washington Yearb.* **79**, 394 (1980).
4. A. C. Sigleo and G. R. Helz, *Geochim. Cosmochim. Acta* **45**, 2501 (1981).
5. G. W. Bailey and J. L. White, *J. Agric. Food Chem.* **12**, 324 (1964).
6. S. W. Karickhoff, D. S. Brown, T. A. Scott, *Water Res.* **13**, 241 (1979).
7. J. C. Means, J. J. Hassett, S. G. Wood, W. L. Banwart, in *Polynuclear Aromatic Hydrocarbons*, P. W. Jones and P. Leber, Eds. (Ann Arbor Science, Ann Arbor, Mich., 1979), pp. 327–340.
8. J. C. Means, S. G. Wood, J. J. Hassett, W. L. Banwart, *Environ. Sci. Technol.* **14**, 1524 (1980).
9. C. T. Chiou, L. J. Peters, V. H. Freed, *Science* **206**, 831 (1979).
10. P. S. C. Rao, J. M. Davidson, V. E. Berkheiser, L. T. Ou, J. J. Street, W. B. Wheeler, T. L. Yuan, *Retention and Transformation of Selected Pesticides and Phosphorus in Soil-Water Systems: A Critical Review* (Environmental Protection Agency, Washington, D.C., in press).
11. T. L. Wu, *J. Environ. Qual.* **9**, 459 (1980).
12. These experiments were supported by Environmental Protection Agency grant R805932. We thank J. J. Cooney and G. R. Helz for their helpful comments on this manuscript. Contribution No. 1231 of the Center for Environmental and Estuarine Studies of the University of Maryland. Work reported here is part of a dissertation to be submitted by R.W. to the graduate school of the University of Maryland for the degree of Ph.D.

3 November 1981

The High-Velocity Core of the Western Boundary Undercurrent at the Base of the U.S. Continental Rise

Abstract. *The Western Boundary Undercurrent is a high-velocity, contour-following bottom current that flows southwesterly on the U.S. Atlantic continental margin. A high-velocity core of the Western Boundary Undercurrent is delineated by an analysis of underlying sediments, which are characterized by coarse particle sizes and efficiently aligned magnetic grains in a zone from 4440 meters at the base of the rise to 5200 meters on the adjacent abyssal plain.*

The Western Boundary Undercurrent (WBUC) is a high-velocity bottom current that flows southwesterly on the continental margin of the eastern United States. This westward-intensified bottom current consists of North Atlantic deep water that is formed in the Norwegian Sea, and it flows as a contour-following current along the continental slope and rise (*1–3*). The WBUC location has traditionally been inferred from current meters and bottom photographs of sea-floor morphology (*4*) on the continental slope and rise. The exact WBUC location and velocity, however, are not well understood. Early studies placed the WBUC at a depth of less than 3000 m (*2*); later studies placed it deeper than 3000 m (*3, 4*), but in none of these studies was the eastern margin of the WBUC identified.

During the last decade studies have suggested that the current is present at a depth from approximately 1500 m to more than 5000 m (*5*). Although the WBUC appears to flow throughout the depth range, the high-velocity core of the WBUC is more restricted. A problem arises, however, because there is no consensus on the definition of the high-velocity WBUC along the continental slope and rise. Fine sediment is transported as a nepheloid layer (*5, 6*), which is intensified along the lower continental rise (*6*). Palynomorphs on the slope and rise are displaced far to the south of probable source areas (*7*) as a result of the southwesterly transport to the WBUC. Recent evidence for the WBUC, however, was found near the base of the Nova Scotian continental rise by investigators of the High-Energy Benthic Boundary Layer Experiment (HEBBLE) (*8*). A combination of sea-floor morphology, nephelometer data, and sedimentary evidence (*9*) was used to infer the location of the WBUC in a region where bottom current meters indicated a bottom current with a velocity as high as 72 cm/sec at a depth of 4988 m (*10*). The upper limit of the high-velocity current is placed at approximately 4500 m (*9*) on the basis of the most shallow occurrence of medium-scale (10-cm) ripples. Small-scale (< 10 cm) ripples were observed on the rise at depths of 4000 to 4500 m (*9*). The results of the HEBBLE study and earlier results indicate that the WBUC resides on the continental slope and rise but apparently has a high-velocity region at depths below 4000 m.

In addition to contourite deposition by the WBUC, other mechanisms may affect deposition on the continental slope and rise. Turbidity currents and shelf-slope spillover may deposit sediment derived from more shallow sources (*11*). Since turbidites are deposited by a down-slope current whereas contourites are deposited by an along-slope current, the direction of transport, as revealed by grain alignment, has been proposed as a means to delineate the two modes (*12*). The assumption of grain alignment parallel to turbidity-current flow (*12*), however, has been challenged by more recent work which shows that grains near the base of a turbidite may be aligned normal to the current as a result of traction transport along the bottom during deposition (*13*). Turbidites on the slope may be restricted to submarine canyons and adjacent spillover areas (*14*). Therefore, we have restricted our study on the slope to intercanyon areas in order to reduce the possibility of encountering turbidites and slump deposits (*15*). Below 4300 m, however, the canyons lose topographic expression, and areas of localized turbidite deposition are difficult to predict.

To our knowledge, none of the earlier investigators of sediments beneath the WBUC (*4–7, 9*) have used parameters that are sensitive to modern benthic oceanography and applicable to relative paleovelocity or paleoposition estimates for the WBUC. We have measured two sedimentological parameters in gravity core-top samples (*16*) from a study area on the continental slope and rise from New Jersey to North Carolina (Fig. 1). These two parameters have been shown to be sensitive to relative bottom-current velocity in deep-sea sediments (*13, 17*); the carbonate-free mean silt size (*18*) and magnetic grain long-axis alignment efficiency (*19*) are independent methods used to identify the location of high-velocity, deep-sea bottom currents.

Figure 2 shows the cross section of

 0036-8075/82/0219-0970$01.00/0

three traverses with the particle size and alignment values plotted above the core position on the profile. We arbitrarily decided that a mean size value of 6.45 ϕ and a particle alignment (F_s) value of 1.03 would be used to separate relatively high- and low-velocity regions. These values were chosen on the basis of results for high- and low-velocity regimes in the Vema Channel (*17, 20*). These values are approximately mean values for the data and give consistent results on the three profiles. The particle alignment parameter has a lower sampling density on the profiles since an undisturbed sample was not available for many cores. Therefore, F_s does not delineate transition zones as sharply as the silt mean.

On two traverses (A–A′ and C–C′) there is a coarsening trend in the silt mean size data from 3000 m to the shallowest core on each profile (Fig. 2). The gradual trend persists up to 2100 m with a dramatic coarsening above this depth. This trend is observed in both of the grain size profiles; however, an associated increase in the magnetic alignment is not observed. The magnetic alignment in the shallowest samples actually remains quite constant at low F_s values. One possible explanation is that the silt mean is more sensitive than the magnetic grain alignment to low bottom-current velocity. Since these depths fall within a zone on the lower slope where low-velocity bottom currents attributed to the WBUC may be found (*5*), this possibility cannot be ignored. Another possible mechanism may be simply a function of proximity to the terrestrial source area; as samples are taken closer to the source, a grain size increase is expected but an associated magnetic alignment increase is not expected since alignment efficiency is independent of proximity to the source. A similar increase in the organic carbon content toward the terrestrial source is observed (*21*), and the organics may have been transported to the shallow continental slope depths by the same processes that provided the coarse silt.

From 2100 to 4400 m, samples are fine-grained with poor alignment values, an indication of low relative bottom-water velocity (Fig. 2). There is some fluctuation in the values within this region, but the dominant trend indicates an area of fine-grained sediment accumulation with poor particle alignment in a zone of low inferred bottom-water velocity. The sharp transition on the silt grain size profile defines the depth to which this low-velocity zone extends. The transition to high velocity occurs at 4460 m on

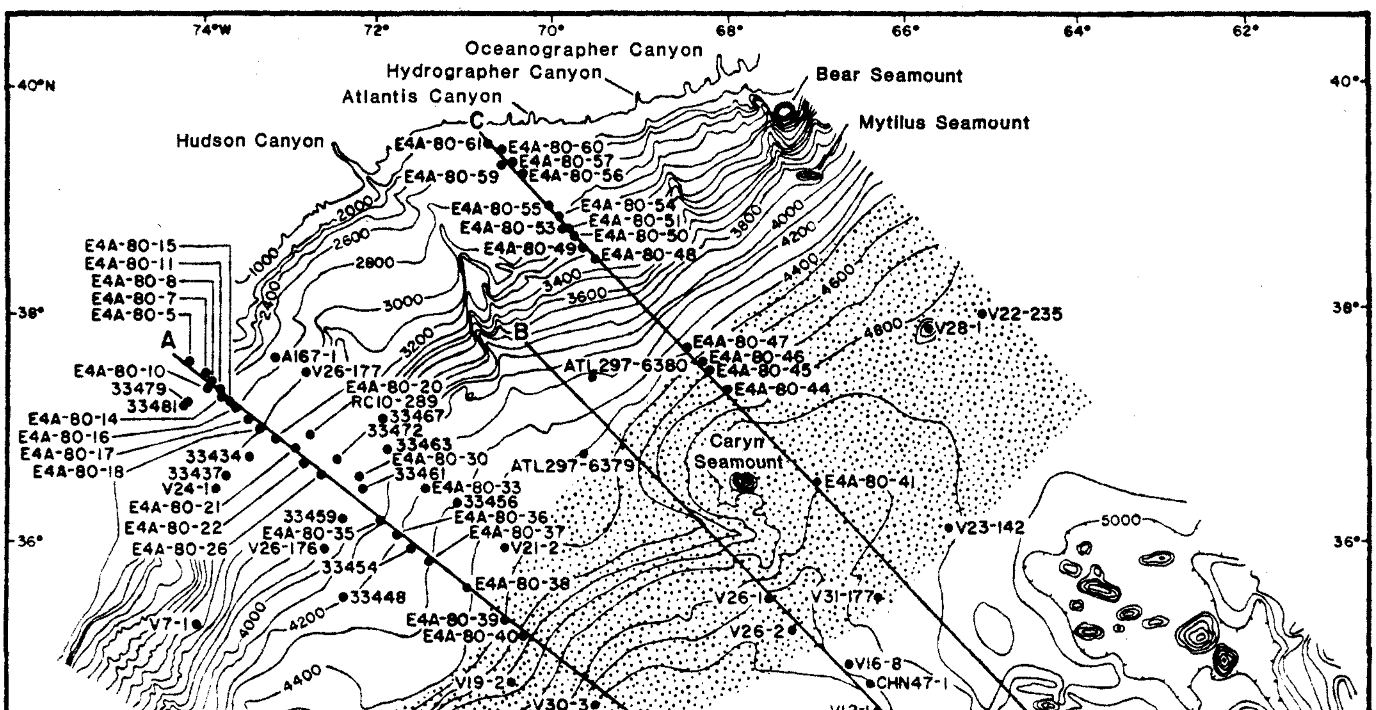

Fig. 1. The bathymetry of the U.S. continental rise from New Jersey to North Carolina is shown with core locations on three profiles (A–A′, B–B′, and C–C′). The shaded area indicates the width (~ 300 km) of the high-velocity core of the Western Boundary Undercurrent determined from this study (see Fig. 2).

profile A–A′, at 4420 on profile C–C′, and at 4300 m on profile B–B′. Because there is a greater concentration of cores on profiles A–A′ and C–C′, we chose an average depth of 4440 ± 20 m as the western (upper) boundary of a high-velocity core of the WBUC.

It is also possible to identify the eastern margin of the high-velocity core of the WBUC on profiles B–B′ and C–C′ (Fig. 2). Profile B–B′ shows that the transition from high to low velocity occurs between cores V26-2 and V16-8, where the sharp change in silt mean values indicates the same magnitude of variation as on the western margin. Silt mean values on profile C–C′ show a decrease at the same distance from the continental rise as on profile B–B′. Although the arbitrary 6.45-ϕ transition line is not actually crossed, there is an abrupt decrease in grain size that is similar to that observed in profile B–B′, an indication that the eastern edge of the high-velocity WBUC is nearby. Profile A–A′ does not show the separation between high and low inferred velocity as accurately as the other profiles because of a lack of samples. The transition may occur at core V30-3, which is at the transition value of 6.45 ϕ, but it is difficult to support the placing of the boundary there on the basis of one data point. Since the two deepest samples (RC3-2 and RC2-5) are extremely fine-grained, the eastern boundary must fall to the west of those sites. The inferred high-velocity region narrows on profile A–A′ if the transitional point at core V30-3 is used to establish the boundary. Additional samples are needed to define the position of the eastern boundary on profile A–A′.

An alternate explanation for the trends in grain size and alignment is deposition by a turbidity current. This mechanism is capable of transporting coarser continental shelf-slope material to great depths, but the evidence appears to be to the contrary. The cores have no megascopic turbidites; the sand fraction reveals low percentages (0 to 7 percent) of quartz sand; the proportion of displaced shallow benthic foraminifera is in quantitatively insignificant amounts. The change from fine to coarse silt mean values occurs on the lower continental rise where the change in slope is minimal, and the location therefore is an unlikely area of turbidite deposition. In addition, the coarsening is observed in profiles A–A′ and C–C′ at nearly identical depths, which is unlikely for widely separated turbidites. Finally, a gradual fining of grain sizes toward the distal end of a turbidite is expected. Instead, particle sizes remain nearly constant, and there is a sharp decrease at the eastern edge with a magnitude similar to that found at the western edge (Fig. 2). Although this evidence does not totally eliminate turbidity currents as a depositional mode on the lower rise, it does favor a contourite depositional mechanism.

We conclude that the silt mean and magnetic alignment parameters define a zone of high-velocity bottom water at the base of the continental rise (Fig. 1), which we ascribe to a high-velocity core of the WBUC. As far as we know, this is the first report that identifies both boundaries of any segment of the WBUC. The western (upper) margin of the high-velocity WBUC is defined by a sharp transition in the silt mean values at a depth of 4440 m. Our placement of the boundary at this depth is consistent with

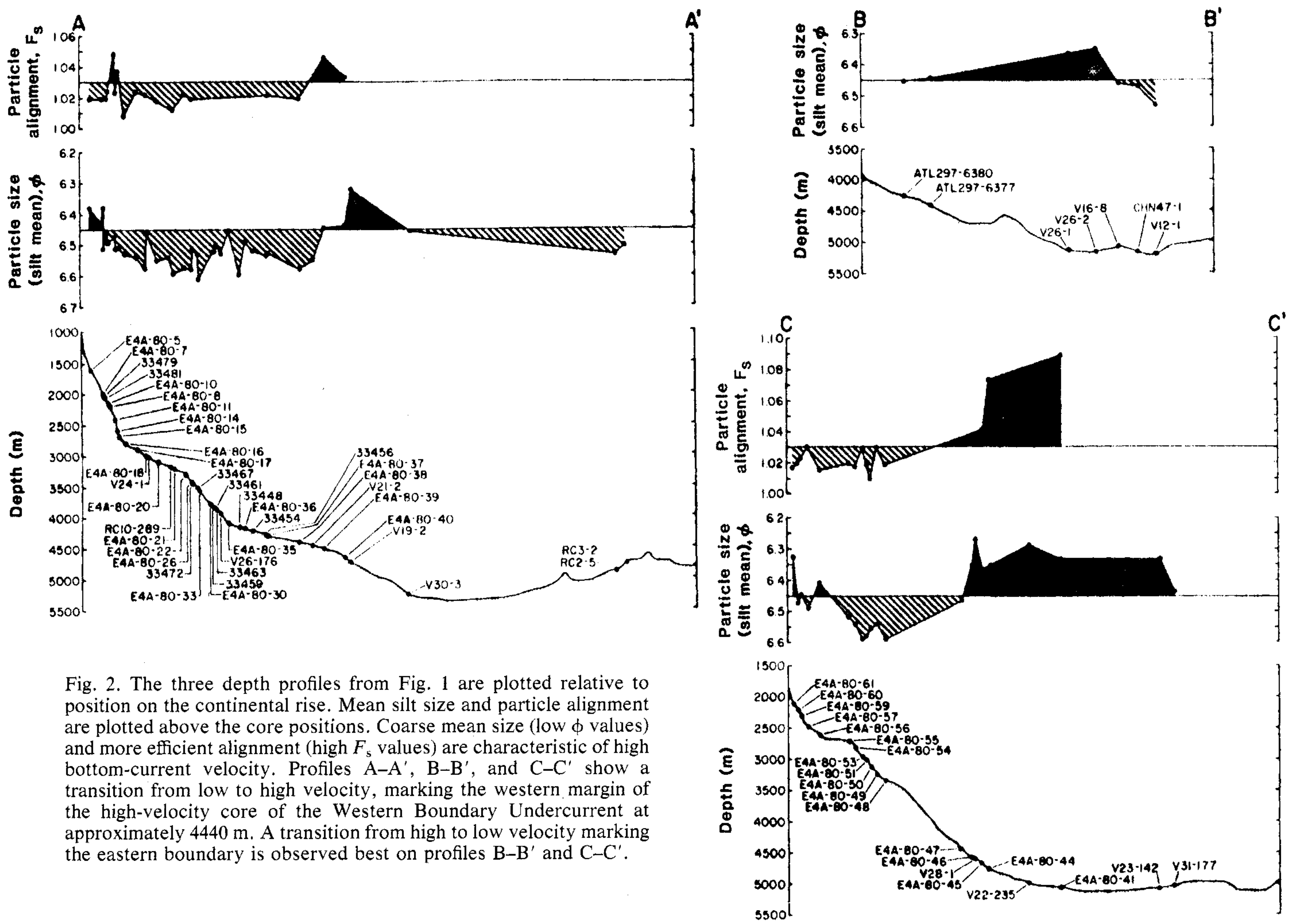

Fig. 2. The three depth profiles from Fig. 1 are plotted relative to position on the continental rise. Mean silt size and particle alignment are plotted above the core positions. Coarse mean size (low ϕ values) and more efficient alignment (high F_s values) are characteristic of high bottom-current velocity. Profiles A–A′, B–B′, and C–C′ show a transition from low to high velocity, marking the western margin of the high-velocity core of the Western Boundary Undercurrent at approximately 4440 m. A transition from high to low velocity marking the eastern boundary is observed best on profiles B–B′ and C–C′.

the observation by HEBBLE investigators of a high-velocity, southward-flowing current deeper than 4000 m with an increased velocity below 4500 m. The highest inferred velocity occurs at approximately 4900 m (Fig. 2), where the highest current velocity in the HEBBLE area was 72 cm/sec (*9, 10*) and the greatest light-scattering in the nepheloid layer is found (*6*). The width of the high-velocity core of the WBUC is approximately 300 km (Fig. 1). The eastern margin of the WBUC core occurs on the abyssal plain at water depths of 5100 to 5400 m and is characterized by a transition in silt mean values similar to that observed on the western margin. The existence of two such well-defined margins may be due to the long residence time of the WBUC core in this channel or to the meandering of the WBUC high-velocity core within this zone during the time represented by the geologic samples. Since our velocity parameters indicate that the margins are quite abrupt, we suggest that the high-velocity WBUC has flowed in a narrow (300 km) channeled area between 4440 and 5200 m for the time represented in our samples (~ 100 to 200 years).

DOUGLAS L. BULFINCH
MICHAEL T. LEDBETTER
BROOKS B. ELLWOOD
Department of Geology,
University of Georgia, Athens 30602
WILLIAM L. BALSAM
Division of Natural Science,
Southampton College,
Southampton, New York 11968

References and Notes

1. L. V. Worthington and G. H. Volkman, *Deep-Sea Res.* **12**, 667 (1965).
2. J. C. Swallow and L. V. Worthington, *ibid.* **8**, 1 (1961); J. R. Barrett, *ibid.* **12**, 173 (1965); P. L. Richardson and J. A. Knauss, *ibid.* **18**, 1089 (1971).
3. H. B. Zimmerman, *J. Geophys. Res.* **76**, 5865 (1971).
4. B. C. Heezen, C. D. Hollister, W. F. Ruddiman, *Science* **152**, 502 (1966); E. R. Schneider *et al.*, *Earth Planet. Sci. Lett.* **2**, 351 (1967); C. D. Hollister and B. C. Heezen, in *Studies in Physical Oceanography*, A. L. Gordon, Ed. (Gordon & Breach, New York, 1972), vol. 2, p. 37.
5. P. R. Betzer, P. L. Richardson, H. B. Zimmerman, *Mar. Geol.* **16**, 21 (1974); G. T. Rowe and R. J. Menzies, *Deep-Sea Res.* **15**, 711 (1968); D. J. Stanley *et al.*, *Mar. Geol.* **40**, 215 (1981); J. C. MacIlvane and D. A. Ross, *J. Sediment. Petrol.* **49**, 563 (1979).
6. S. Eittreim, M. Ewing, E. M. Thorndike, *Deep-Sea Res.* **16**, 613 (1969); P. E. Biscaye and S. L. Eittreim, *Mar. Geol.* **23**, 155 (1977).
7. H. D. Needham, H. Habib, B. C. Heezen, *J. Geol.* **77**, 113 (1969); L. E. Heusser, *Geol. Soc. Am. Abstr. Programs* **9**, 1014 (1977).
8. C. D. Hollister and I. N. McCave, *Eos* **61**, 1015 (1980).
9. B. E. Tucholke, C. D. Hollister, P. E. Biscaye, *ibid.*, p. 1015; P. E. Biscaye, W. D. Gardner, R. J. Zaneveld, H. S. Pak, B. E. Tucholke, *ibid.*, p. 1015; A. N. Shor and B. E. Tucholke, *ibid.*, p. 1015.
10. M. J. Richardson and M. Wimbush, *ibid.*, p. 1015; ______, L. Mayer, *Science* **213**, 887 (1981).
11. K. P. Emery and E. Uchupi, *Mem. Am. Assoc. Pet. Geol.* *17* (1972).
12. D. A. V. Stow, *Sedimentology* **26**, 371 (1979); ______ and J. P. B. Lovell, *Earth Sci. Rev.* **14**, 251 (1979).
13. M. T. Ledbetter and B. B. Ellwood, *Mar. Geol.* **37**, 245 (1980); A. Taira and P. A. Scholle, *Geol. Soc. Am. Bull.* **90**, 952 (1979).
14. M. E. Field and O. H. Pilkey, *J. Sediment. Petrol.* **41**, 526 (1971); J. A. Klasik and O. H. Pilkey, *Mar. Geol.* **19**, 69 (1975).
15. R. W. Embley, *Mar. Geol.* **38**, 23 (1980).
16. Most samples were taken within 4 cm of the core top of large-diameter gravity cores taken aboard the R.V. *Eastward*. The remaining samples were taken within 4 cm of the core top of trigger-weight and gravity cores from existing collections. No attempt was made to verify that core tops represent recent sediments since we are interested in detecting conditions that persist on the present sea floor. Naturally, sediment beneath the high-velocity WBUC will be a lag deposit containing older, reworked material, but the presence of this material indicates the present hydrodynamic environment. Cores shown on Fig. 1 but not on Fig. 2 were analyzed for particle size, but the data are not shown since those cores are near large slump deposits (*15*).
17. M. T. Ledbetter and D. A. Johnson, *Science* **194**, 837 (1976); B. B. Ellwood and M. T. Ledbetter, *ibid.* **203**, 1335 (1979); ______, D. A. Johnson, *Mar. Geol.* **33**, M51 (1979).
18. The noncarbonate fraction in the silt size range from 4 to 8 φ or 62 to 4 μm is isolated, and the mean size is determined by analysis of the particle size distribution with an Elzone (Particle Data, Inc.) electronic sensing instrument [see (*13*) and (*17*) for analytical methods]. The particle size analysis is restricted to the noncarbonate fraction in order to eliminate the effects of carbonate dissolution on the size distribution, so that only effects produced by the bottom current will prevail. The silt size range only is analyzed since those sizes are most sensitive to winnowing by bottom currents with a velocity common in the modern ocean.
19. One determines the magnetic grain long-axis alignment by measuring the anisotropy of magnetic susceptibility (AMS) on a torsion fiber magnetometer. A standardized AMS parameter, F_s, is sensitive to the efficiency of long-axis alignment [see (*13*) and (*17*) for analytical methods]. More efficient alignment is interpreted as evidence of increased bottom-current velocity.
20. C. R. Blaeser, thesis, University of Georgia (1981).
21. W. L. Balsam, L. DuBois, M. Butterworth, E. Halter, R. Karp, S. M. Stedmen, G. Vassilev, *Geol. Soc. Am. Abstr. Programs* **13**, 122 (1981).
22. We thank M. Ayers and A. McIntyre for providing samples. Samples from Lamont-Doherty Geological Observatory were maintained under National Science Foundation (NSF) grant DES72-01568 and Office of Naval Research grant N00014-75-C-0210; support for R.V. *Eastward* samples was provided by NSF grant OCE77-23278A02. This research was supported in part by the Climate Dynamics Program, Division of Atmospheric Sciences, under NSF grant ATM-7817854. L. DuBois (Southampton College) analyzed the benthic foraminifera.

10 September 1981; revised 26 October 1981

Survival and Differentiation of Identified Embryonic Neurons in the Absence of Their Target Muscles

Abstract. *Although prevented from contacting their target muscles, identified limb-innervating neurons in grasshopper embryos survive and differentiate to maturity.*

The survival and differentiation of motoneurons and autonomic neurons in vertebrates are influenced decisively by the cells their axons contact during development; deprived of their target muscles, these neurons usually die (*1*). Central neurons in insects are arranged in ganglia, each of which corresponds to and innervates a particular body segment. Thoracic segments have limbs and their ganglia contain limb-innervating neurons; these cells are absent from ganglia in the abdominal segments, which lack limbs. During embryogenesis, motoneurons in each segment send axons to the periphery to innervate developing muscles, and shortly thereafter many neurons die (*2, 3*). The mechanisms that regulate the survival and differentiation of these insect neurons are unknown. Here we report experiments in which limb buds were removed from insect embryos early in development. Our results show that two identified insect neurons need not contact their target muscle in order to survive and differentiate.

We removed limb buds from early embryos of the grasshoppers *Locusta migratoria* and *Schistocerca americana*. For our experiments in *Locusta* we chose the largest limb motoneuron, the fast extensor tibia (Feti) (*4*), which innervates the extensor tibia muscle of the metathoracic leg. Since Feti sends an axon to only one leg, we removed the metathoracic leg on one side and used the homologous cell on the unoperated side as a control. For our experiments in *Schistocerca* we chose the largest modulatory neuron, the dorsal unpaired median extensor tibia (Dumeti) (*5*), which also innervates the extensor tibia muscle. Since the axon of Dumeti bifurcates and extends into both metathoracic legs, we removed these legs and used the homologous cell from unoperated animals as a control. Both Feti and Dumeti can be recognized in normal embryos by the large size and position of the cell bodies and by their axonal and dendritic morphology (Figs. 1 and 2).

In experiments with *Locusta*, the limb buds were removed from embryos within the egg (*6*). The damage caused by the operation varied. In some cases proximal fragments of the leg remained, and these animals were later rejected. In others the leg was completely removed (serial sections of animals 2 to 3 days after the operation confirmed that no limb muscles were present on the operated side). Sixty-two successful operations were performed; in 25 the limb bud was removed at or before the appearance of